The Analysis and Comparison of Actual to Predicted Collector Array Performances

The Hottel-Whillier-Bliss (HWB) equation has been the standard tool for the evaluation of collector thermal performance for four decades. This paper presents a technique that applies the criteria of ASHRAE Standard 93-77 to the determination of the HWB equation coefficients from field-derived data. Results of the analysis of a sample collector array illustrate the technique. Actual dynamic performances of various collector arrays in the field are compared to those predicted by the steady-state efficiency models for the individual panels. In certain cases, the HWB model produces deviations of over 100% from measured hourly performances and 35% from measured monthly performances when compared with the single-panel laboratory-derived model. However, when the field-derived HWB model is used as the basis of comparison the performance deviations were typically less than 5%.

Introduction

In designing solar energy systems (*e.g.*, heating, cooling, and hot-water applications to residential, commercial, and industrial facilities), the designer usually relies upon published instantaneous efficiency curves for individual collector panels. However, the performance of collector arrays differs from that of a panel since under dynamic conditions the steady-state panel efficiency curve does not adequately represent the collector array performance.

The National Solar Energy Demonstration Program [1] is collecting and archiving data measured for numerous operating solar energy systems. The availability of these data provides an opportunity to verify the practicality of design concepts and tools which previously were considered to be in the province of laboratory scientists. One such tool is the industry standard collector model, the Hottel-Whillier-Bliss (HWB) equation.

This paper presents a technique by which the field performances of collector arrays are related to the HWB equation via ASHRAE Standard 93-77 [2], which established technical criteria for collector evaluation. We show that field data, when subjected to quasi-steady-state constraints, verify the laboratory-derived steady-state collec-

tor efficiency curve for a number of collector types and array manifolding designs [3]. A sample array, located in the north central Great Plains area, is used to illustrate the technique.

This paper also presents a technique for comparing dynamic performance to predicted performance. The results of several collector comparisons are given.

Steady-state collector array efficiency

The steady-state thermal performance of a single flatplate collector is well understood, and has been the subject of a number of technical papers over the past four decades [4-9]. Rigorous thermal performance calculations involve the iterative solution of nonlinear matrix equations of fifth or higher rank. To avoid this complexity, the solar energy industry has adopted the Hottel-Whillier-Bliss equation as its standard tool for steadystate collector evaluation:

$$Q_{\rm u} = F_{\rm R} A_{\rm p} [I(\tau \alpha)_{\rm e} - U_{\rm L} (T_{\rm f,i} - T_{\rm a})]. \tag{1}$$

The elements of the HWB equation are the absorber plate area A_p , the insolation intensity I, the effective product $(\tau \alpha)_a$ of the cover transmissivity and the plate absorptiv-

Copyright 1979 by International Business Machines Corporation. Copyring is permitted without payment of royalty provided that (1) each reproduction is done without alteration and (2) the *Journal* reference and IBM copyright notice are included on the first page. The title and abstract may be used without further permission in computer-based and other information-service systems. Permission to *republish* other excerpts should be obtained from the Editor.

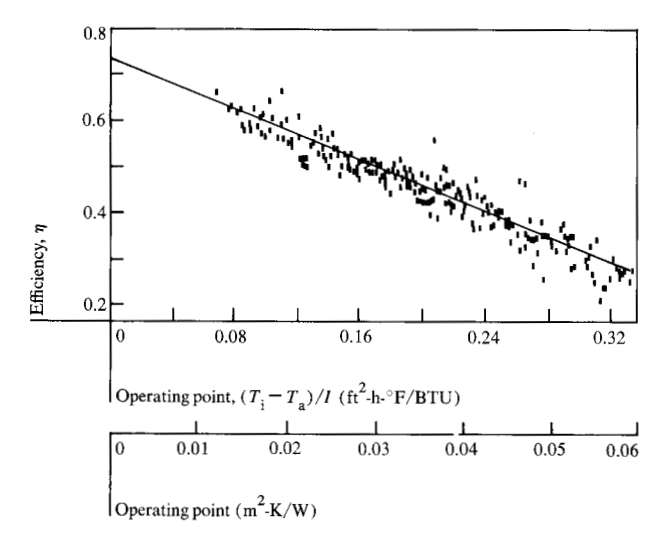


Figure 1 Typical instantaneous efficiency curve as drawn from actual test data. The operating point is defined as $(T_{\rm f,i}-T_{\rm a})/I$.

ity, the collector loss coefficient $U_{\rm L}$, the transport fluid inlet temperature $T_{\rm g}$, the external ambient temperature $T_{\rm a}$, and a collector heat removal factor $F_{\rm R}$.

The principal inaccuracy of the HWB equation lies in the assumption that $U_{\rm L}$ is constant; in reality, it is highly dependent upon wind and temperature. The usual method for collector evaluation is to set up steady-state laboratory test conditions and measure the rate of thermal energy gain $Q_{\rm u}$ from the equation

$$Q_{\rm u} = \dot{m}c_{\rm p}(T_{\rm f,e} - T_{\rm f,i}),\tag{2}$$

where \dot{m} is the transport fluid mass flow rate, $c_{\rm p}$ is the specific heat of the transport fluid, and $T_{\rm f,e}$ is the temperature of the transport fluid as it exits from the collector. By setting Eqs. (1) and (2) equal and then solving for the ratio of actual energy collected $Q_{\rm u}$ to the incident energy IA, where A is the gross collector area (instead of the absorber area $A_{\rm p}$), the instantaneous efficiency equation is derived:

$$\eta = Q_{\rm u}/IA$$

$$= F_{\rm R}(\tau\alpha)_{\rm e} - F_{\rm R}U_{\rm L}(T_{\rm f,i} - T_{\rm a})/I.$$
(3)

Since $Q_{\rm u}$ from Eq. (2) and $(T_{\rm f,i}-T_{\rm a})/I$ (the operating point of the system) can be determined from measurable quantities, only $F_{\rm R}(\tau\alpha)_{\rm e}$ and $F_{\rm R}U_{\rm L}$ remain unknown. A plot of η (ordinate) vs the operating point $(T_{\rm f,i}-T_{\rm a})/I$ (abscissa) is the instantaneous efficiency curve, and yields a straight line with an intercept value of $F_{\rm R}(\tau\alpha)_{\rm e}$ and a slope equal to $-F_{\rm R}U_{\rm L}$. Such a curve is usually published

by the manufacturer of a solar collector and this curve is used by system designers to predict array performances.

Collector testing guidelines based on ASHRAE Standard 93-77 were adopted by the solar energy industry to help provide a convenient but consistent basis for comparison of various collectors and collector configurations. Briefly described, it was required that all testing be accomplished under the following five conditions:

- A steady-state collector temperature environment,
- ◆An insolation intensity greater than 200 BTU/ft²-h (630 W/m²),
- ◆ A wind speed of less than 10 mph (4.5 m/s),
- ◆ A range of ambient temperature of less than 55°F (13°C),
- A minimum of 16 efficiency points required.

Thus, the test method of ASHRAE 93-77 involves first establishing steady-state conditions of flow, irradiation, exit temperature, and ambient temperature for several values of inlet temperature (the controlled variable). The efficiency values η are then calculated from Eq. (3) and the results plotted (see Fig. 1), using a first-order, least-squares curve fit.

The extension of single collector performance expectations to collector arrays composed of multiple solar panels requires certain assumptions, since the single collector analysis does not consider the working fluid held in the external manifolding and risers. For an array of more than one or two collectors, the energy flow in the transport fluid held external to the panel becomes significant.

It should also be noted that the ASHRAE steady-state requirement is equivalent to requiring a zero propagation time between a change in fluid-inlet conditions and the effect on the fluid-outlet conditions. Because actual operating collector arrays are exposed to a variety of dynamic forcing functions (clouds, wind, diurnal variations in sunlight, shade, etc.), the expectation is that steady-state conditions will never be observed. Although good manifolding designs and proper insulation would minimize the effects of such functions, the question remains as to how well any steady-state curve can model the long-term performance of collector arrays under dynamic conditions.

The major effect of the fluid mass between inlet and outlet temperature sensors is to delay the propagation of transient effects, resulting in a large degree of scatter in the derived information points. To partially compensate for this effect, the energy-gain equation is modified to include stored, internal energy.

Consider implementation of the ASHRAE collector thermal analysis procedure in a system that acquires time-coherent (all quantities measured simultaneously) data points at equally spaced intervals. (In the paper, a time-coherent group of measurements is called a scan.) The measured parameters are the fluid volumetric flow-rate \dot{W} , the fluid exit temperature $T_{\rm f,e}$, the fluid inlet temperature $T_{\rm f,i}$, the ambient temperature $T_{\rm a}$, and the insolation level I (intensity). The fluid specific heat $c_{\rm p}$ may be calculated from its material properties. The fluid mass M between the inlet and outlet temperature sensors is a measured constant. The volumetric flowrate \dot{W} is converted to mass flowrate \dot{m} through multiplication by the fluid density ρ and the flow-correction factor $f_{\rm c}$ [10]. For computation of the operating point (the abscissa) we write

$$X = (T_{\rm fi} - T_{\rm a})/I; \tag{4}$$

for computation of the ordinate we write

$$\eta = \dot{m}c_{\rm p}(T_{\rm f.e.} - T_{\rm f.i})/IA + Mc_{\rm p}(\Delta T_{\rm avg})/IAt, \tag{5}$$

where $\Delta T_{\rm avg}$ is the change in the average fluid temperature over the scan period t.

Recall that although the use of Eqs. (4) and (5) assumes steady-state thermal conditions, the field-derived measurements are dynamic and include transient thermal effects. Therefore, constraints must be placed on the field-derived data in order to meet the steady-state requirements of ASHRAE 93-77 and to obtain the HWB equation. These constraints typically take the form of limitations on the magnitude and allowable variation in the data with time. The application of such constraints is referred to as *filtering*.

Filtering

The filtering process attempts, as closely as practical, to adhere to the philosophy and procedures outlined in ASHRAE Standard 93-77. To accomplish this, eight filters were designed to effectively impose and implement the restrictions associated with quasi-steady-state operating conditions. The limiting filters are presented first.

• Sun angle maximum

The sun angle constraint is required in order to exclude reflection effects at low angles of incidence and to compensate for collector array orientations that do not face due south. When flat-plate collectors are evaluated, it is desirable to exclude all data points beyond 30° of the collector normal. However, tracking collectors and tubular collectors operate well at higher angles, and the sun angle filter limit is increased correspondingly.

• Insolation floor

The insolation floor filter establishes a variable lower limit on the incident sun intensity. It is nominally set for 200 BTU/ft²-h (630 W/m²), but may be adjusted as required for the collector array design.

• Wind velocity ceiling

We have placed a ceiling on the wind velocity. Recall that the principal sources of error in the HWB equation were based on variations of $U_{\rm L}$ with wind and temperature. Since the wind filter is adjustable in the software system we use, the exact effect on $U_{\rm L}$ may be characterized for a given array. Such control of the wind effects reduces the point scatter considerably.

The variation filters are listed below, and the capability is provided for choosing the number of scans (time-coherent groups of measurements, e.g., at a 320-second period) over which the variation constraints are imposed.

- Insolation variation between scans,
- Inlet temperature variation between scans,
- Temperature gain variation between scans,
- Ambient temperature variation between scans,
- Flowrate variation between scans.

After the raw scan data have passed the limiting filters, the search begins for steady-state conditions. Examination of Eqs. (4) and (5) reveals that the flow, the fluid inlet and exit temperatures, the ambient temperature, and the insolation level enter into the determination of a point on the operating point- η coordinate system. These are the measurements that must be held nearly constant for a period of time greater than the time constant of the collector in order to establish steady-state conditions.

Example results of different collector array types

We have applied this technique to thermal performance analyses of three quite different solar collector arrays.

• Aluminum-absorber copper-tube collector array
Figure 2(a) is the initial scatter diagram derived by applying Eqs. (4) and (5) to raw, unfiltered data from an aluminum-absorber copper-tube collector array (glass glazing).
Application of a 10-mph (4.5-m/s) ceiling on the wind velocity reduces the scatter to a much narrower band, as shown in Fig. 2(b). Figure 2(c) is the scatter diagram of the points remaining after setting the sun angle filter to 30° and the variation filters to 5% over one 320-second scan. A regression line has been plotted through the points, from which the slope and intercept values are found to be -0.303 and 0.815, respectively.

• Lexan-glazed aluminum-absorber steel-tube collector array

Figure 3(a) is the initial scatter diagram for a Lexanglazed aluminum-absorber steel-tube collector array with no filtering. Figure 3(b) is the efficiency curve derived from the raw data by using the same filtering process

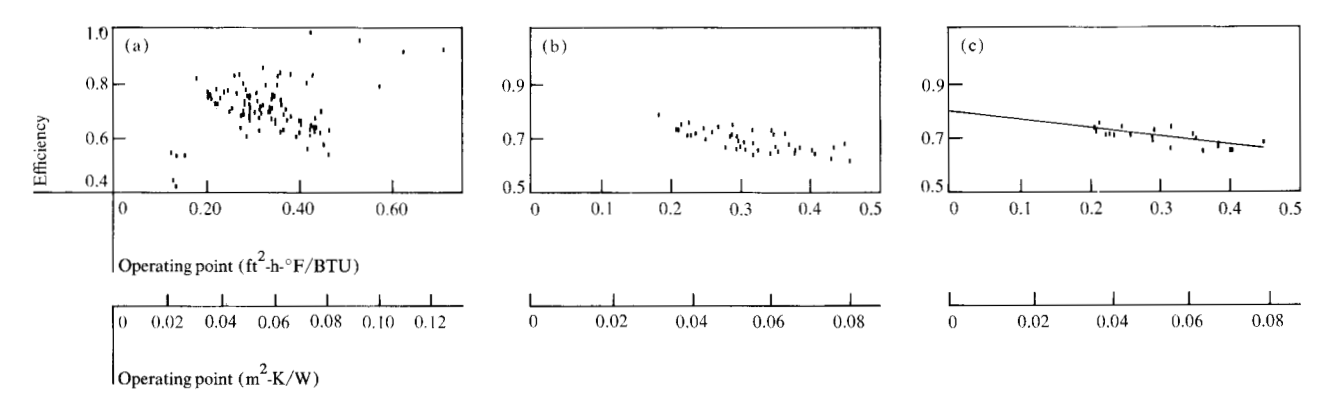


Figure 2 Instantaneous efficiency curves for an array of aluminum-absorber copper-tube collectors. (a) Scatter diagram with all filters open. (b) Improved scatter diagram obtained with wind filter limited to 10 mph (45 m/s). (c) Further improved diagram obtained when all filter variations were limited to 5%; the sun angle to \leq 30°; insolation, to \geq 200 BTU/ft²-h (630 W/m²); and wind speed to \leq 10 mph (4.5 m/s). The slope ($-F_RU_L$) equals -0.303, the intercept equals 0.815.

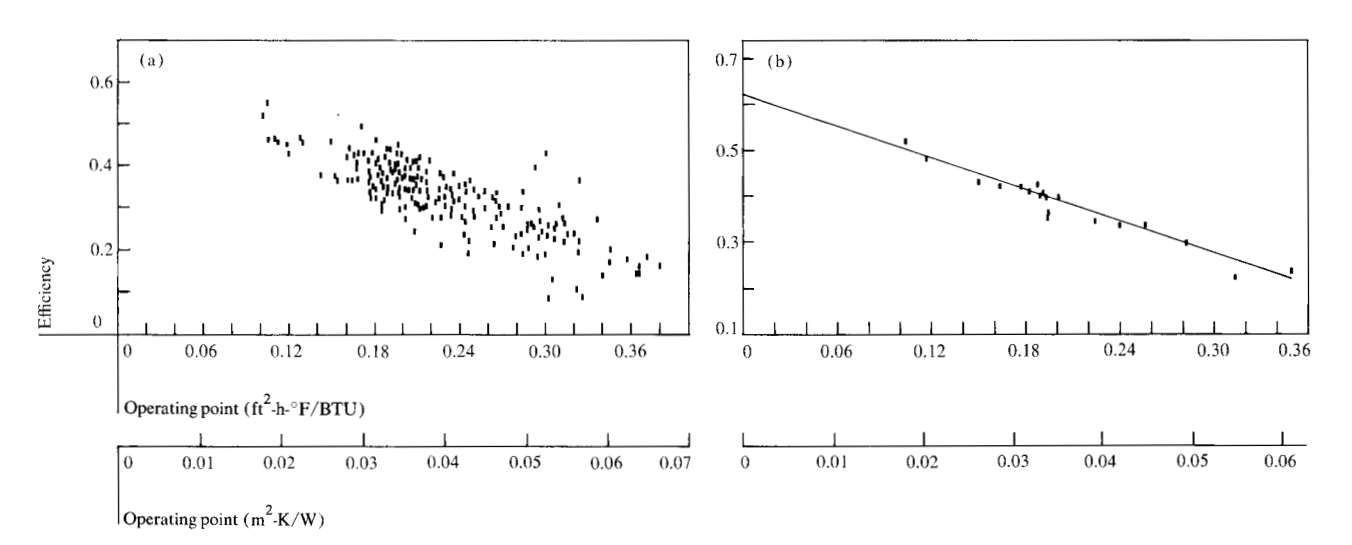


Figure 3 Scatter diagram for an array of Lexan-glazed aluminum-absorber steel-tube collectors. (a) All filters open; the slope equals -1.127, the intercept equals 0.592. (b) All filter variations limited to 5%; the sun angle to \leq 30°; insolation to \geq 200 BTU/ft²-h (630 W/m²); and the wind speed to \leq 10 mph (4.5 m/s). The slope ($-F_RU_L$) equals -1.146, the intercept equals 0.621.

mentioned above and by curve fitting. Note that the coefficients obtained from the filtered and unfiltered data show deviations of less than 5%.

• Fresnel lens tracking concentrating collector array
Figure 4 is the final scatter diagram for an array of Fresnel
lens tracking concentrating collectors. It was not possible
to reduce the point scatter beyond that shown with the
standard filters. In these situations, the collector analysis
tool may be used to diagnose probable causes of nonconvergence by an iterative selection of filter settings.
This particular array was found to be primarily influenced
by wind velocity, which, it is postulated, may induce
tracking errors or greater heat losses in the manifolding.

The abundance of raw data available from solar energy demonstration systems permits reference of field performance to the HWB equation. The technique presented allows for reduction of scattered operating points to a data set that is consistent with the requirements of ASHRAE 93-77. The HWB model thus obtained provides engineers, designers, architects, contractors, and other interested persons with a model that is representative of the design's performance, and which may then be incorporated into future designs and cost trade analyses.

Comparison of actual to predicted array performances

The HWB model obtained from field measurement may also be compared to the predicted performance or con-

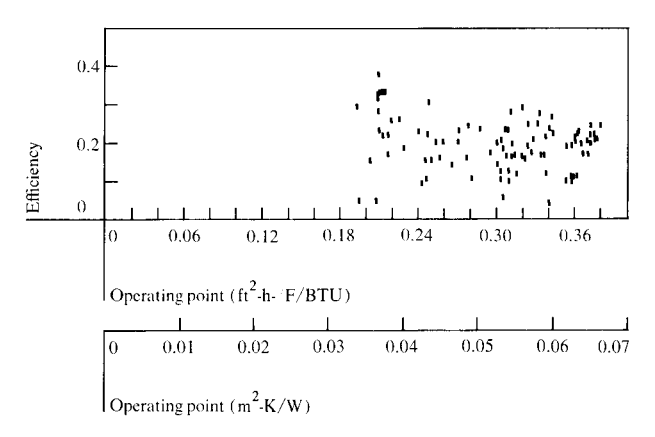


Figure 4 Scatter diagram for an array of Fresnel lens tracking concentrating collectors.

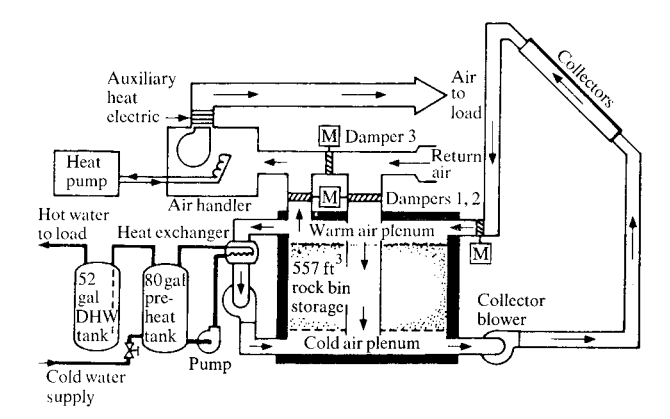


Figure 5 Schematic representation of the System A solar energy system.

Table 1 Collector array performance for System A.

Month		Collector efficiency			
	Incident	Incident oper.	Collected	Array	Operational
March	16.752 (17.673)*	14.799 (15.613)	5.906 (6.231)	0.35	0.40
April	20.558 (21.689)	18.656 (19.682)	6.755 (7.127)	0.33	0.36
May	17.290 (18.241)	15.441 (16.290)	4.891 (5.160)	0.28	0.32
June	21.236 (22.404)	19.407 (20.474)	5.487 (5.789)	0.26	0.28
July	20.138 (21.246)	18.332 (19.340)	4.931 (5.202)	0.24	0.27
August	21.032 (22.189)	19.500 (20.573)	5.267 (5.557)	0.25	0.27
	117.006 (123.441)*	106.135 (111.972)*	33.237 (35.065)*	0.29†	0.32†

^{*}Given in units of 109 J. †Average values.

trolled test performance data available for various collector components. This comparison allows for a more accurate estimate of the collector area required to satisfy particular design loads, and should ultimately help in minimizing the cost of the solar energy systems. The technique can also provide information on the impact of environmental conditions (e.g., sensitivity to wind) on the performance of collector arrays. The next section of this paper presents detailed comparisons between the actual collector array performances and those predicted by the HWB model for six active solar energy systems. The collector performance evaluations of these systems will be presented individually. These systems are all part of the National Solar Heating and Cooling Demonstration Program [1].

System A

• System description

The site is a single-family residence in Canton, Ohio. The system is designed to provide approximately 50% of the space heating and 70% of the DHW requirements. It has

an array of flat-plate collectors [Solar Energy Products Co. (SEPCO), Avon Lake, Ohio; ROM-AIRE EF-212] with a gross area of 436 ft² (40.5 m²). The array faces south at an angle of 37° from the horizontal. Air is used as the medium for delivering solar energy from the collector array to storage. Solar energy is stored in a bin containing 5.01×10^4 lbs (22.7 Mg) of rock. The solar heated air, passing through a heat exchanger, also preheats incoming city water, which is stored in an 80-gallon (0.30-m³) preheat storage tank and supplied, on demand, to a conventional 52-gallon (0.20-m³) DHW tank. When solar energy is insufficient, a liquid-to-air heat exchanger within a 2.5ton (1 ton of air conditioning is equivalent to 12 000 BTU/ h or 3.5 kW) heat pump and a three-stage electric heater in the air handling unit provide additional energy for space heating. An electric heating element in the 52-gallon (0.20-m³) DHW tank provides auxiliary energy for water heating. The system, shown in Fig. 5, has four modes of operation:

- Collector to space heating,
- Collector to storage,

257

Table 2 Energy gain comparison for System A for the month of August 1978; calculated parameters: $F_{\rm R}(\tau\alpha)_{\rm e}=0.59, -F_{\rm R}U_{\rm L}=-1.054;$ SEPCO ROM-AIRE EF-212 collectors.

Day	Energy gai	$n (10^6 \text{ BTU})$	Error (10 ⁶ BTU)	Percent deviation
	Predicted	Actual	(IO BIO)	aeviation
1	0.305976	0.205397	-0.100579	-32.8
2	0.324714	0.207000	-0.117714	-36.3
3	0.073634	0.052163	-0.021471	-29.2
4	0.329000	0.240030	-0.088970	-27.0
5	0.100903	0.082417	-0.018486	-18.3
6	0.033233	0.031847	-0.001386	- 4.2
7	0.111635	0.081224	-0.030411	-27.2
8	0.310827	0.212147	-0.098680	-31.7
9	0.270573	0.177562	-0.093011	-34.4
10	0.136227	0.106771	-0.029456	-21.6
11	0.156171	0.135041	-0.021130	-13.5
12	0.173809	0.145376	-0.028433	-16.4
13	0.402699	0.293353	-0.109346	-27.2
14	0.282877	0.208473	-0.074404	-26.3
15	0.231635	0.159611	-0.072023	-31.1
16	0.095101	0.059309	-0.035792	-37.6
17	0.378807	0.256860	-0.121947	-32.2
18	0.292601	0.199407	-0.093194	-31.9
19	0.232646	0.144266	-0.088380	-38.0
20	0.320861	0.239736	-0.081125	-25.3
21	0.402517	0.295118	-0.107399	-26.7
22	0.313456	0.231836	-0.081620	-26.0
23	0.282560	0.190371	-0.092189	-32.6
24	0.164854	0.117282	-0.047572	-28.9
25	0.164480	0.132048	-0.032432	-19.7
26	0.281661	0.212994	-0.068667	-24.4
27	0.132168	0.093718	-0.038450	-29.1
28	0.124785	0.080183	-0.044602	-35.7
29	0	0	0	0
30	0	0	0	0
31	0	0	0	0
	6.430492 (6.784169)*	4.688326 (4.946184)*	-1.742166 (-1.837985)*	-27.1†

^{*}Given in units of 109 J.

- Storage to space heating,
- Domestic water preheat.

The installation was in continuous operation during the six months from March to August of 1978. Data collected over this period were used for the performance evaluation. The complete system-wide thermal performance is presented in Ref. [11]. Detailed monthly performance reports are given in Ref. [12].

• Collector array performance

Measured monthly values of incident and collected solar energies and the collector array efficiencies are presented in Table 1. The collector operational efficiencies are determined from the actual conditions of all-day solar energy systems operation. Measured monthly values of operational incident energy and computed values of operational collector efficiency are also given in the table. (Operational incident solar energy is that part of the daily energy available to the collector while the transport fluid is circulating.)

The collector array consists of 16 SEPCO ROM-AIRE EF-212 units and two reduced-area units equivalent to a seventeenth unit in area, manifolded in parallel. Figure 6(a) presents a histogram of the collector operating points for August and Table 2 presents a daily energy-gain comparison between the actual energy gain and that predicted by the single-panel laboratory HWB curve. From these data it can be concluded that the actual performance was consistently lower than that predicted by about 27%. The placement of the blower upstream of the collector array results in the discharge of heated air around the collector seals, which contributes to this lowered efficiency.

The average monthly operational collector efficiency was 0.32. The efficiency was higher in the spring, and decreased as the summer season advanced. This represents a migration of the collector operating point toward higher positive values, and is due to an increase in the average collector inlet temperature. This is consistent with the observation that storage became more fully charged as the season advanced, creating higher inlet temperatures.

Referring again to Fig. 6(a), two curves are plotted in the operating-point histogram. The solid line is the HWB curve derived from laboratory tests; the broken line is the HWB curve derived from field measurements on the collector array. An energy-gain comparison to the field-derived curve results in a +9.4% error. Contrasting this result with the -27.1% error obtained from the comparison to the laboratory single-panel curve implies that a significant bias results from the array effects of this installation.

System B

System description

The site is an industrial laundry in Fresno, California with an average hot water demand of over 30 000 gallons (115 m³) per day at a demand temperature of 180°F (82°C). The solar energy system is designed to provide the preheating for this water.

The collector array consists of 140-flat plate, Lexanglazed collectors (SP4120), manufactured and installed by the Ying Manufacturing Co., Gardena, California. The collectors are single-glazed, with an aluminum absorber plate painted flat black. The back of the collector array is insulated with one inch of polyurethane foam and the sides with one inch of polyurethane foam. The collector

[†]Average value.

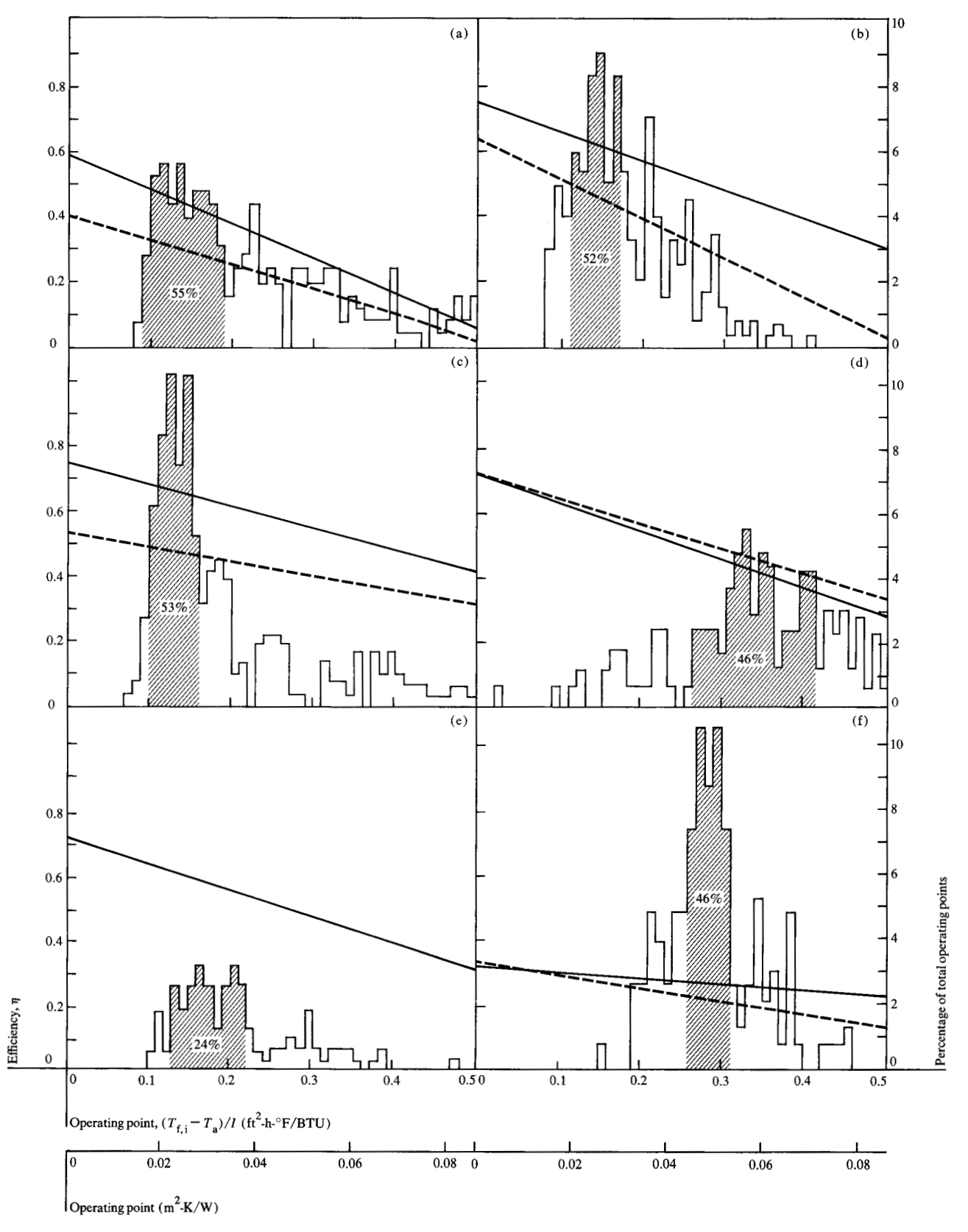


Figure 6 The operating point histograms and collector efficiency performance curves [laboratory-predicted single-panel HWB (—) and field-derived (----)] for Systems (a) A, (b) B, (c) C, (d) D, (e) E, and (f) F. The right-hand ordinate gives the percentage of operating points (histogram). The percentage of operating points falling within the shaded portion of each histogram is also indicated.

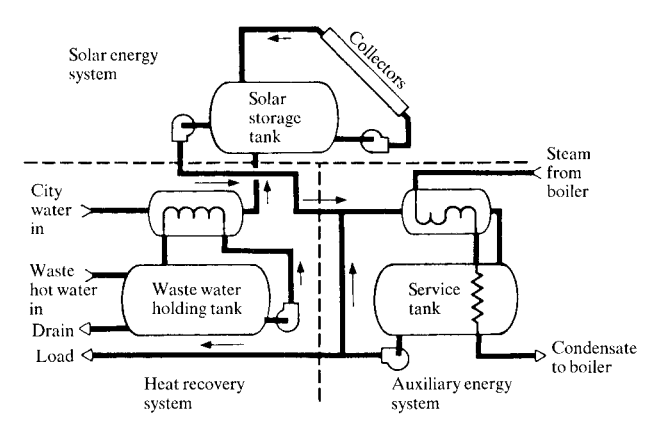


Figure 7 Schematic representation of the System B solar energy system.

piping is insulated with one inch of fiberglass insulation. Although there are no measured data to calculate the actual losses between the collectors and storage, these losses are believed to be insignificant because of the insulated pipes and the relatively short distance of ≈75 ft (23 m) between the collectors and storage. Water is the medium used to deliver solar energy from the collector array to storage. The heated water is stored in a 12 500-gallon (47-m³) tank. When solar energy is insufficient, auxiliary energy is supplied by a low-pressure, gas-fired boiler. Also, a heat exchanger utilizing energy from a waste-water storage tank provides additional energy to the city water input supply. The system, shown schematically in Fig. 7, has three modes of operation:

- Collector to storage,
- Hot water demand,
- Storage to waste water.

Detailed reports on the system are available from Refs. [13, 14]. It should be noted that the hot water load is the load on the solar energy system after the load has been reduced by the heat-recovery system.

• Collector array performance

Measured monthly values of incident and collected solar energies and the collector array efficiencies are presented in Table 3. In addition, the table lists the amount of solar energy incident on the array when water was being circulated through the collectors. The ratio of this energy to the solar energy collected is used to determine the efficiency of the array when the solar collection system was operational. Table 3 shows that the average operational efficiency of the collectors during the reporting period was 0.37. This value is slightly less than expected based on the manufacturer's data. There are several possible reasons:

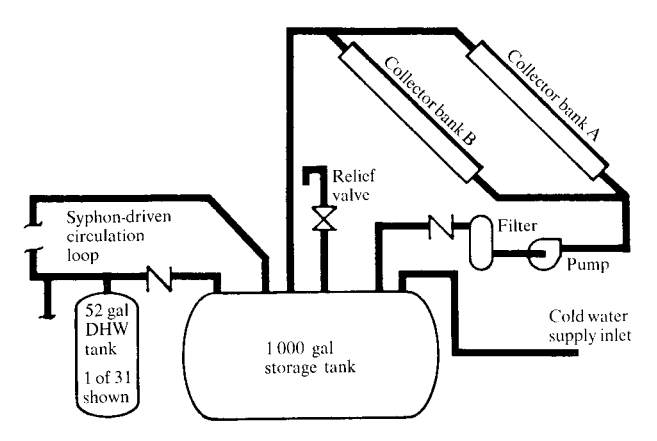


Figure 8 Schematic representation of the System C solar energy system.

- The collector fluid flow rate is only 1.5 gallons per minute $(9.5 \times 10^{-5} \text{ m}^3/\text{s})$ through each collector, while the optimal flow rate is 2.5 gallons per minute $(1.6 \times 10^{-4} \text{ m}^3/\text{s})$.
- Communication with the manufacturer indicates that the collectors may be dirty and should be washed several times per month.

A detailed analysis of the performance in August shows that the system operated for 52% of the time between operating points of 0.12 and 0.18 ft²-h-°F/BTU (0.021 and 0.032 m²-K/W); [see Fig. 6(b)]. Table 4 shows a consistent daily deviation from the predicted value, which is clustered about the mean monthly percent deviation of -27.8%. In other words, the system performance, on the average, was 27.8% poorer than predicted. By using the tabular data and noting the narrow range of operating points, we conclude that the actual average performance curve can be drawn through the point where $\eta = 0.43$ and $(T_{\rm f,i} - T_{\rm a})/I = 0.15$ ft²-h-°F/BTU (0.026 m²-K/W).

If the field-derived HWB model [broken line in Fig. 6(b)] is used as the basis of comparison, the error is reduced to +2%. This leads to two observations: The error between the single-panel laboratory predicted energy gain and the actual energy gain is primarily bias; and dynamic operating conditions for the installation have minimal impact on the collector array performance. The point $\eta = 0.43$, $(T_{\rm f,i} - T_{\rm a})/I = 0.15$ ft²-h-°F/BTU falls on the field-derived HWB curve.

System C

• System description

The project provides hot water preheating to a threestory, 31-unit condominium located in San Diego, Califor-

Table 3 Collector array performance for System B.

Month		Solar energy (10 ⁶ BTU)		Collector efficiency	
	Incident	Incident oper.	Collected	Array	Operational
Nov. 77	253 (267)*	190 (200)*	89 (94)*	0.35	0.47
Dec. 77	144 (152)	82 (87)	31 (33)	0.21	0.38
Jan. 78		<u> </u>		_	_
Feb. 78	184 (194)	131 (138)	41 (43)	0.22	0.31
March 78	261 (275)	195 (206)	69 (73)	0.26	0.35
April 78	302 (319)	234 (247)	80 (84)	0.27	0.34
May 78	419 (442)	259 (273)	94 (99)	0.22	0.37
June 78	403 (425)	302 (319)	99 (104)	0.25	0.33
July 78	410 (433)	235 (343)	117 (123)	0.30	0.36
August 78	406 (428)	302 (319)	122 (129)	0.30	0.40
	2782 (2935)*	2020 (2131)*	742 (783)*	0.26†	0.37†

^{*}Given in units of 109 J.

nia. The system has $520 \text{ ft}^2 \text{ (48 m}^2\text{) of double-glazed flat-plate collectors.}$

The collector array consists of three banks of 14, 10, and 4 panels (Revere Copper and Brass, Rome, New York) interconnected by long runs of piping. The individual panels are each equipped with uninsulated isolation valves on the inlet and outlet. The largest contributors to energy losses within the collector subsystem appear to be the long pipe runs and the uninsulated isolation valves.

Potable water is used as the medium for transferring solar energy from the collector array to a 1000-gallon (3.8-m³) buried storage tank. The storage tank is glass lined and insulated with two inches of polyurethane foam. A siphon-driven circulation loop delivers preheated water from the storage tank to individual domestic hot water (DHW) tanks in each of the 31 units. Each unit is provided with a conventional electric immersion heater to boost the inlet water temperature to the level required for usage. The system is described in Fig. 8. There are no heat exchangers in the system, since the working fluid is potable water (San Diego seldom experiences freezing weather). The system has been designed for two modes of operation:

- Collector to storage,
- Storage to DHW tanks.

The system provided 37% of the domestic hot water energy requirements for the 31-unit condominium. However, only 61% of the energy collected arrived at the load, which is equivalent to 24% of the available solar energy. (For a detailed report of the total system performance see Ref. [15].) Losses between the collector and storage were typically 6.5×10^5 BTU $(6.9 \times 10^8 \text{ J})$ per month; losses

Table 4 Energy gain comparison for System B for the month of August 1978; calculated parameters: $F_{\rm R}(\tau\alpha)_{\rm e}=0.717, -F_{\rm R}U_{\rm L}=0.871;$ Ying SP4120 collectors.

Day	Energy ga	in (10 ⁶ BTU)	Error (10 ⁶ BTU)	Percent deviation
	Predicted	Actual	, ,	
1	7.478586	5.145726	-2.332860	-31.2
2	5.985734	4.118141	-1.867593	-31.2
3	7.778229	5.791701	-1.986528	-25.5
4	4.527383	3.016701	-1.510682	-33.4
5	4.459995	2.651670	-1.808325	-40.5
6	0	0	0	0
7	7.038310	5.089183	-1.949127	-27.7
8	6.992405	5.224766	-1.767639	-25.3
9	6.765580	5.016459	-1.749121	-25.8
10	7.228387	5.336887	-1.891500	-26.2
11	5.849702	4.111454	-1.738248	-29.7
12	4.245401	2.727651	-1.517750	-35.8
13	1.677077	0.804822	-0.872255	-52.0
14	7.013862	5.155397	-1.858466	-26.5
15	7.170570	5.369806	-1.800764	-25.1
16	6.962114	5.147749	-1.814365	-26.1
17	6.785951	4.769010	-2.016941	-29.7
18	7.057284	5.032863	-2.024421	-28.7
19	4.953790	2.812626	-2.141164	-43.2
20	0	0	0	0
21	0	0	0	0
22	6.649286	4.459451	-2.189835	-32.9
23	6.890683	4.861343	-2.029340	-29.5
24	5.848967	4.083357	-1.765610	-30.2
25	7.832182	5.342833	-2.489349	-31.8
26	4.540270	2.551634	-1.988636	-43.8
27	1.001175	0.440603	-0.560572	-56.0
28	6.899604	5.042840	-1.856764	-26.9
29	6.843704	5.041114	-1.802590	-26.3
30	6.795973	4.848954	-1.947019	-28.6
31	5.697103	4.020001	-1.677102	-29.4
	168.969000	121.948000	-47.021307	
	(178.26200)*	(128.655000)*	(-49.607478)*	

^{*}Given in units of 10° J.

[†]Average values.

[†]Average values.

Table 5 Collector array performance for System C.

Month		Solar energy (10 ⁶ BTU)		Collector efficiency	
	Incident	Incident oper.	Collected	Array	Operational
March	23.56 (24.86)*	20.25 (21.36)*	11.76 (12.41)*	0.50	0.58
April	25.66 (27.07)	21.89 (23.09)	11.90 (12.55)	0.46	0.54
May	26.18 (27.62)	22.79 (24.04)	12.41 (13.09)	0.47	0.54
June	24.32 (25.66)	21.31 (22.48)	9.54 (10.06)	0.39	0.45
July	25.23 (26.62)	22.64 (23.88)	10.03 (10.58)	0.40	0.44
August	27.18 (28.67)	24.41 (25.75)	10.46 (11.04)	0.39	0.43
	152.13 (160.50)*	133.29 (140.62)*	66.10 (69.74)*	0.44†	0.50†

^{*}Given in units of 109 J.

Table 6 Energy gain comparison for System C for the month of August 1978; calculated parameters: $F_{\rm R}(\tau\alpha)_{\rm e}=0.73, -F_{\rm R}U_{\rm L}=0.64$; Revere collectors.

Day	Energy gai	$n (10^6 \text{ BTU})$	Error (10 ⁶ BTU)	Percent deviation
	Predicted	Actual	(IV BIO)	aeviation
1	0.507110	0.367989	-0.139121	-27.4
2	0.415067	0.359982	-0.154085	-30.0
3	0.433421	0.305281	-0.128140	-29.6
4	0.476016	0.329879	-0.146137	-30.7
5	0.520746	0.364559	-0.156187	-30.0
6	0.457699	0.323681	-0.134018	-29.3
7	0.518704	0.361026	-0.157678	-30.4
8	0.341249	0.227238	-0.114011	-33.4
9	0.431535	0.316349	-0.115186	-26.7
10	0.468562	0.329185	-0.139377	-29.7
11	0.309223	0.224906	-0.084317	-27.3
12	0.470016	0.331567	-0.138449	-29.4
13	0.508812	0.356879	-0.151933	-29.9
14	0.515887	0.368808	-0.147079	-28.5
15	0.523347	0.345097	-0.178250	-34.0
16	0.506602	0.335142	-0.171460	-33.8
17	0.512730	0.332329	-0.180401	-35.2
18	0.565272	0.374208	-0.191064	-33.8
19	0.447684	0.315347	-0.132337	-29.5
20	0.516891	0.345068	-0.171823	-33.2
21	0.515292	0.363727	-0.151565	-29.4
22	0.579288	0.380260	-0.199028	-34.3
23	0.563668	0.373358	-0.190310	-33.7
24	0.552274	0.367961	-0.184313	-33.3
25	0.587585	0.399667	-0.167918	-29.5
26	0.623992	0.417934	-0.206058	-33.0
27	0.547645	0.387107	-0.160538	-29.3
28	0.368390	0.254839	-0.113851	-30.8
29	0.262813	0.196054	-0.066759	-25.4
30	0.462611	0.321372	-0.141239	-30.5
31	0.560807	0.380172	-0.180635	-32.2
	15.170000	10.457000	-4.713000	-31.1†
	(16.000000)*	(11.032000)*	$(-4.972000)^*$	

^{*}Given in units of 10° J.

from the buried storage tank were typically 2.1×10^6 BTU $(2.2 \times 10^9 \text{ J})$ per month. [The storage tank is buried in the ground and occasionally the local water table is above the storage tank; this contributes to the relatively high (20%) storage losses.] The losses between storage and the individual DHW tanks were typically 1.3×10^6 BTU per month. These high transport losses (13%) can be attributed to the long pipe runs to the individual DHW tanks. During extended periods when the system is not used the water does not circulate and this standing water then cools. Other sources of heat loss are early morning control instability and the long collector-to-storage pipe runs.

• Collector array performance

The measured monthly values of incident and collected solar energies and the collector array efficiencies are listed in Table 5.

Collector array efficiency may be viewed from two perspectives. The first assumes that the efficiency is based on all available solar energy; however, that point of view makes the operation of the control system a part of the array efficiency. For example, energy may be available at the collector but the collector fluid temperature is below the control minimum; thus, the energy is not collected. The monthly efficiency computed by this method is listed in the collector array efficiency column.

The second viewpoint assumes that the efficiency is based on only the incident energy during periods of collection. The monthly efficiency computed by this method is listed in the operational collector efficiency column.

The average operational efficiency of the collector array during the report period was 50%. The operational

[†]Average values.

[†]Average value.

collector efficiency was lower in the summer months when higher storage temperatures were maintained, and the operating point was forced to higher levels (driven to the right) on the collector instantaneous efficiency curve. Figure 6(c) shows such a curve for the month of August. Fifty-three percent of the operating points lie between 0.1 and 0.16 ft^2 -h-°F/BTU (0.017 and 0.028 m²-K/W). In addition to the discussion above, the operating points to the right reflect the influence of the increased late afternoon storage temperatures; this is consistent with low afternoon utilization of the hot water. By using the data shown in Table 6 and Fig. 6(c), and the narrow range of operating points, it is shown that the point $\eta = 0.44$ and operating point = $0.13 \text{ ft}^2\text{-h-}^\circ\text{F/BTU}$ (0.023 m²-K/W) lies on the field-derived performance curve (see dotted line). The monthly deviation between the actual and predicted energy gains was -31.1%, and the average daily error was $-1.52 \times 10^{5} \text{ BTU } (-1.60 \times 10^{8} \text{ J}); i.e.$, the system array performance was 31.1% poorer than predicted.

If the field-derived performance curve is used to predict energy gain the error is reduced to +2.2%. As in the case of System B, the difference between the actual energy gain and that predicted by the laboratory-derived single-panel curve appears to be largely due to bias, with little error being attributable to dynamic effects.

System D

• System description

The system is installed in a 1548-ft² (144-m²), three-bedroom, single-family dwelling, located in Winter Springs, Florida. The system is designed to provide solar energy for space heating and cooling and for domestic hot water heating. Solar energy is collected by two banks of doubleglazed, flat-plate collectors (Chamberlain 711301) with a gross area of 714 ft² (66 m²); these are manufactured by the Chamberlain Manufacturing Corporation, Elmhurst, Illinois. These panels are divided into two banks and are mounted on the south roof of the house at a tilt angle of 18° from the horizontal in order to optimize collection for cooling. Solar energy is transferred from the collector array to a 1350-gallon (5.1-m³) underground storage tank. Water is used as the medium for collection, transfer, and storage of heat. Space heating demands are met by circulating water from storage through heating coils in the air distribution system of the house. Auxiliary space heating is provided by a natural-gas-fired boiler. A 3-ton (10.5kW) solar-energy-powered absorption cycle water chiller provides chilled water for circulation through the same air distribution system. A gas-fired boiler will provide supplemental thermal energy to the chiller when sufficient thermal energy is not available from storage. Solar energy for heating domestic hot water is provided by circulating

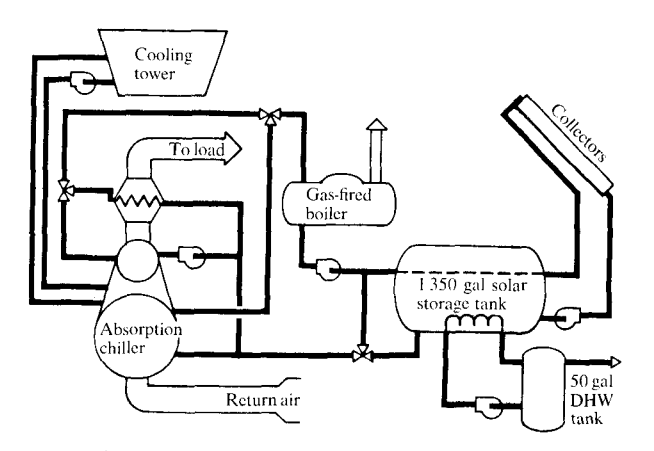


Figure 9 Schematic representation of the System D solar energy system.

water from a conventional 50-gallon (0.2-m³) domestic hot water heater through a double heat exchanger located in the solar storage tank. Auxiliary energy for domestic hot water is provided by natural gas whenever the temperature of the hot water tank falls below 130°F (54-55°C). The system, shown schematically in Fig. 9, has the following modes of operation:

- Collector to storage,
- Space heating from storage,
- Space cooling from storage,
- Domestic hot water heating,
- Excess heat rejection.

The performance of the system was evaluated from May to August, 1978. The daily and monthly performance factors, as well as a more complete system thermal performance evaluation, can be obtained from References [16, 17], and are used in the following evaluation. During this period, the system collected 3.54×10^7 BTU $(3.73 \times 10^{10} \text{ J})$ of the 1.42×10^8 BTU $(1.50 \times 10^{11} \text{ J})$ incident on the collector array. The solar energy system provided 41% of the space cooling demand and supplied 100% of the energy needed to maintain the temperature (160°F or 71°C) of the domestic hot water tank. There was no demand for space heating during this period.

Solar energy supplied 40% of the energy required to meet the space cooling demand during this period. These 1.82×10^7 BTU $(1.92 \times 10^{10} \text{ J})$ were delivered to the generator of the absorption cycle water chiller and resulted in a production of 8×10^6 BTU $(8.4 \times 10^9 \text{ J})$ of cooling. An additional 2.67×10^7 BTU $(2.82 \times 10^{10} \text{ J})$ of auxiliary energy were consumed to provide the remainder of the space cooling demand.

Table 7 Collector array performance for System D.

Month		Solar energy (10 ⁶ BTU)				
	Incident	Incident oper.	Collected	Array	Operational	
May	30.118 (31.774)*	27.330 (28.833)*	9.464 (9.985)*	0.24	0.35	
June	33.857 (35.719)	20.717 (21.856)	9.021 (9.517)	0.27	0.44	
July	31.809 (33.558)	19.688 (20.771)	7.660 (8.080)	0.24	0.39	
August	37.616 (39.685)	25.931 (27.357)	9.229 (9.737)	0.25	0.36	
	133.400 (140.736)*	93.666 (98.818)*	35.374 (37.320)*	0.25†	0.38†	

^{*}Given in units of 109 J.

Table 8 Energy gain comparison for System D for the month of August 1978; calculated parameters: $F_{\rm R}(\tau\alpha)_{\rm e}=0.692, -F_{\rm R}U_{\rm L}=0.557;$ Chamberlain 711301 collectors.

Day	Energy gair	n (10 ⁶ BTU)	Error (10 ⁶ BTU)	Percent deviation
	Predicted	Actual	(,	
1	0.027875	0.059351	0.031476	112.9
2	0	0	0	0
3	0.033023	0.040118	0.007095	21.5
4	0.095406	0.138179	0.042773	44.8
5	0	0	0	0
6	0.056893	0.087173	0.030280	53.2
7	0.081418	0.121749	0.040331	49.5
8	0.037814	0.068452	0.030638	81.0
9	0.049214	0.110719	0.061505	125.0
10	0.066506	0.091061	0.024555	36.9
11	0.526713	0.492588	-0.034125	- 6.5
12	0.212898	0.192530	-0.020368	- 9.6
13	0.308337	0.313969	0.005632	1.8
14	0.286191	0.284714	-0.001477	- 0.5
15	0.410334	0.398128	-0.012206	- 3.0
16	0.592372	0.543887	-0.048485	- 8.2
17	0.440102	0.411808	-0.028294	- 6.4
18	0.358690	0.320430	-0.038260	-10.7
19	0.424677	0.381793	-0.042884	-10.1
20	0.447586	0.376197	-0.071389	-15.9
21	0.559658	0.510203	-0.049455	- 8.8
22	0.457364	0.438424	-0.018940	- 4.1
23	0.399664	0.393469	-0.006195	- 1.6
24	0.329821	0.359571	0.029740	9.0
25	0.601450	0.499657	-0.101793	-16.9
26	0.630443	0.581969	-0.048474	- 7.7
27	0.563279	0.494002	-0.069277	-12.3
28	0.554471	0.486681	-0.067790	-12.2
29	0.532956	0.519096	-0.013860	- 2.6
30	0.259004	0.240085	-0.018919	- 7.3
31	0.333469	0.273605	-0.059864	-18.0
	9.677638	9.229608	-0.448030	- 4.6†
	(10.209908)*	(9.737236)*	$(-0.472672)^*$	

^{*}Given in units of 109 J.

• Collector array performance

Table 7 summarizes the performance of the collector array for the reporting period from May to August, 1978. When based on the total incident solar energy, the aver-

age collector array efficiency was 25%. However, the operational collector efficiency was much closer to the efficiency quoted by the collector manufacturer than that for any other collector evaluated by us. The average operational collector efficiency was 38%. The operational efficiencies during May were much lower than this average because of the high storage tank temperatures that resulted from the continued collection of solar energy without using that energy to power the absorption cycle chiller (until May 16). During August the operational efficiency was again slightly reduced due to a control-system anomaly that restricted the flow through the collectors when the collection pump was on. Cooling system operational anomalies during both July and August resulted in higher storage tank temperatures, and thus reduced the operational efficiency.

The detailed analysis for August is shown in Table 8 and in Fig. 6(d). It can be seen that the array operated predominantly in the operating point region between 0.26 and 0.47 ft²-h-°F/BTU (0.046 and 0.083 m²-K/W), which is indicative of a high storage temperature. This is expected for a system that provides energy to the generator of an absorption chiller. The tabular data indicate a monthly error of -4.6%. That is, the actual energy gain was 4.6%less than the predicted energy gain over the month of August. Examination of the daily values indicates deviations between +125% and -18%. The majority of the positive deviations occurred on days when energy collection was very low, which implies overcast conditions and a high ratio of diffuse to direct sunlight. It is seen that the laboratory-derived HWB model is appropriate for this application of this particular collector. The field-derived curve is seen to deviate very slightly from the laboratory-derived curve.

System E

• System description

The system, located in Washington, DC, has two banks of Sunworks Inc. (New Haven, Connecticut) liquid Solector

[†]Average values.

[†]Average values

flat-plate collectors, used to support energy requirements for a hot water system. The two banks contain 302 panels and have a gross area of 6254 ft² (531 m²). The restaurant requires approximately 7000 gallons (26.5 m³) of hot water each day between 4 pm and 2 am. This hot water is used by the restaurant's kitchen facilities and must be supplied at 150°F (65-66°C). The solar energy system is a retrofit, and as such, the collectors face southwest instead of the ideal south. The solar collector loop uses a 60/40 solution of propylene glycol/water as the heat transfer fluid. The potable water supply is isolated from the heat exchange fluid by a liquid-to-liquid heat exchanger. The collection and transfer of solar energy are controlled by the activation of two sets of pumps (see Fig. 10). When the difference between control temperature measurements located near instrumentation measurements T102 and T205 exceeds an "activate" setting in the controller, the primary pump of the (P1, P2) pair is turned on. The other pump is a backup pump that starts automatically if the primary pump fails. These pumps alternately change roles and are interlocked to prevent both from running simultaneously. The second set of pumps (P3, P4) is similarly configured and is activated whenever set (P1, P2) is turned on. Solar heated water is stored in two 5000-gallon (19-m³) tanks. Additional heating of service hot water is accomplished by a 9.6×10^5 -BTU/h (2.8×10^5 -W) gasfired boiler. The system was designed for three modes of operation:

- Hot water demand,
- Collector to storage with hot water,
- Regenerate.

The performance was evaluated for the period from June to August of 1978. A more complete, system-wide thermal performance evaluation and detailed monthly data for this facility can be found in Refs. [18, 19]. The average monthly thermal load was 1.30×10^8 BTU $(1.37 \times 10^{11} \text{ J})$, 64% of which was supplied by the solar energy system.

• Collector array performance

The monthly values of incident and collected solar energies and the collector array efficiencies are listed in Table 9. The average collector array performance based on the gross collector area of 6254 ft² (581 m²) was 34%. Actually, however, 33 of the panels were inoperative during the reporting period; therefore, the incident solar energy reported in the table must be corrected by approximately 11%, and the collector array efficiency shown must be likewise corrected. The average corrected collector array efficiency was 38%. Thus, the actual performance of the working panels was slightly better than that predicted by the manufacturer.

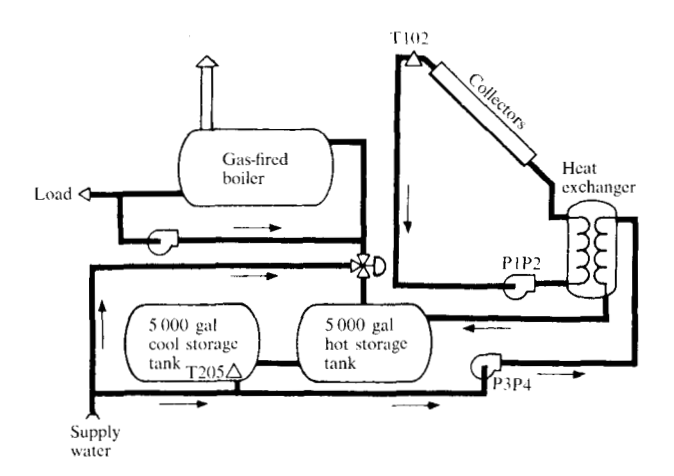


Figure 10 Schematic representation of the System E solar energy system.

Table 9 Collector array performance for System E.

Month	Solar energ	Collector array efficiency	
	Incident	Collected	
June	276.50 (291.71)*	94.62 (99.82)*	0.34
July	253.29 (267.22)	85.63 (90.34)	0.34
August	246.39 (259.94)	86.07 (90.80)	0.35
	776.18 (818.87)	266.32 (280.97)	0.34†

^{*}Given in units of 109 J.

Analysis for the month of June showed an energy imbalance between the collector loop and the storage tank; *i.e.*, more energy was being stored than was being collected. Subsequent investigation indicated that the transport fluid, which should have been 60/40 propylene glycol/water, had actually been diluted to 30/70 by the frequent addition of water. Since the specific heat of the transport fluid is used to compute the amount of energy collected, any variation from the specified propylene glycol concentration will cause errors in this computed value, and in the corresponding collector array performance factors. The difference between the actual and assumed specific heat of the transport fluid was 10%, and this difference would account for the observed energy imbalance.

The detailed analysis of the month of August was used to draw the histogram shown in Fig. 6(e) (see Table 10 for daily data). The operating points were widely spread. Twenty-four percent of the operating points fell between 0.13 and 0.22 ft²-h-°F/BTU (0.039 m²-K/W). The data

[†]Average value.

Table 10 Energy gain comparison for System E for the month of August 1978; calculated parameters: $F_{\rm R}(\tau\alpha)_{\rm e}=0.73, -F_{\rm R}U_{\rm L}=0.83;$ Sunworks liquid Solector collectors.

Day	Energy gain	(10 ⁶ BTU)	Error (10 ⁶ BTU)	Percent d	eviation
	Predicted*	Actual	,	Uncorrected	Corrected
1	0.582828	0.998151	0.415283	71.2	92.4
2	1.849135	1.742945	-0.106318	- 5.7	5.9
3	2.663288	2.400943	-0.262528	- 9.9	1.3
4	0.235969	0.485702	0.249733	105.8	131.3
5	4.914226	4.017143	-0.897083	-18.3	- 8.2
6	2.554054	2.327860	-0.226194	- 8.9	2.4
7	3.626022	3.163182	-0.462840	-12.8	2.0
8	2.548837	2.686622	0.137785	5.4	18.4
9	2.537228	2.499398	-0.037830	- 1.5	10.7
10	3.353743	3.090851	-0.262892	- 7.8	3.6
11	4.364658	3.706010	-0.658648	-15.1	- 4.6
12	2.361327	2.361664	0.000337	0	12.4
13	0.276364	0.371880	0.095516	34.6	51.2
14	2.536959	2.140640	-0.396319	-15.6	- 5.2
15	3.328916	2.922203	-0.406713	-12.2	- 1.4
16	4.884370	4.098951	-0.785419	-16.1	- 5.7
17	4.528482	4.071822	-0.456660	-10.1	1.0
18	4.702676	4.318909	-0.383787	- 8.2	3.2
19	4.404490	3.787964	-0.616526	-14.0	- 3.4
20	4.277816	3.877337	-0.400484	- 9.4	1.8
21	4.567544	4.087670	-0.479874	-10.5	0.6
22	4.387115	3.885507	-0.501608	-11.4	- 1.6
23	4.653479	4.062680	-0.590799	-12.7	- 1.9
24	4.248972	3.928508	-0.320464	- 7.5	3.9
25	2.276477	1.996867	-0.279610	-12.3	- 1.4
26	2.869081	2.429541	-0.439540	-15.3	- 4.9
27	1.674113	1.368997	-0.305116	-18.2	- 8.1
28	3.212410	2.645928	-0.566482	-17.6	- 7.5
29	4.318379	3.685270	-0.633109	-14.7	- 4.1
30	2.011299	2.037875	0.026576	1.3	2.4
31	0.767369	0.875871	0.108502	14.1	28.0
	95.518000 (100.771000)†	86.075000 (90.809000)†	-9.443000 (-9.962000)†	- 9.9 ‡	1.3‡

^{*}Assuming all panels were operative. In actuality 33 of the 302 panels were inoperative. †Given in units of $10^9~\rm J$.

Table 11 Collector array performance for System F.

Month		Solar energy (10 ⁶ BTU)					fficiency
	Inc	rident	Incident oper,	Col	llected	Array	Operational
March	174.43	(184.02)*	118.08 (124.57)*	28.30	(29.86)*	0.16	0.24
April	232.13	(244.90)	184.19 (194.32)	37.60	(39.67)	0.16	0.20
May	221.92	(234.13)	142.60 (150.44)	37.27	(39.32)	0.17	0.26
June	196.11	(206.90)	106.58 (112.44)	19.40	(20.47)	0.10	0.18
July	184.01	(194.13)	122.07 (128.78)	25.09	(26.47)	0.14	0.21
August	203.78	(214.99)	133.76 (141.12)	32.06	(33.82)	0.16	0.24
	1212.38	(1279.06)*	807.28 (851.68)*	179.72	(189.60)*	0.15†	0.22†

^{*}Given in units of 109 J.

given in Table 10 show that the monthly energy gain was 9.9% lower than predicted. This takes into account that 11% of the panels (33 of 302) were actually inoperative.

The daily errors are not consistent, with most large positive errors occurring on days of low energy gain. When the energy gain was very high, say, greater than

[‡]Average values.

 4.0×10^6 BTU (4.2×10^9 J), the errors were negative, but of approximately the same magnitude. This implies a better percent conversion of diffuse compared to direct sunlight.

System F

• System description

The site is a two-story, 5625-ft² (522-m²) concrete block office building located in Buena Vista, Florida. Its solar energy system is designed to provide space heating and cooling, and heating of domestic hot water.

The system employs the only concentrating collector array examined in this paper. The collector subsystem consists of an array of parabolic-trough concentrating collectors with tracking absorber tubes that form an integral part of the building's roof. These were manufactured by the Aircraft Armament Industries (AAI) Corp., Baltimore, Maryland, and have a concentration ratio of 8 to 1. The array is oriented with its major axis in an east-west direction. Sixteen panels, forming an integral part of the office building, are mounted horizontally. The absorber tubes are supported at each end by rocker arms and are interconnected horizontally by I-beam struts forming a parallelogram. The system is focused by an array of solar sensors located on the first absorber tube. An electric motor receives a signal from this focusing device and the motor drives a lead screw that causes the absorber tubes to track the diurnal motion of the sun in a north-south direction. The total collection aperture area is 3840 ft² (357 m²). The trough of each panel consists of a metal frame supporting the individual mirror strips, which are attached to it with mastic. The absorber is composed of copper tubing mechanically attached to an aluminum plate that is painted with black epoxy paint. A single selective glazing covers this component, and the entire assembly is encased in foam insulation and covered with aluminum.

Water is used as the heat collection, transfer, and storage medium. Collected solar energy is stored in a 10 000-gallon (38-m³) hot water tank. Domestic hot water (DHW) is provided by a heat exchanger immersed in the tank. Space heating is provided by the circulation of hot water from the storage tank through heat exchangers located in the central air distribution system. No auxiliary energy is provided for either DHW or for space heating.

A 25-ton (87.5-kW) absorption cycle water chiller, requiring water temperatures in excess of 170°F (77°C), utilizes hot water from storage to provide chilled water to a 10 000-gallon (38-m³) cold water storage tank. For space cooling, water from this cold tank is circulated through

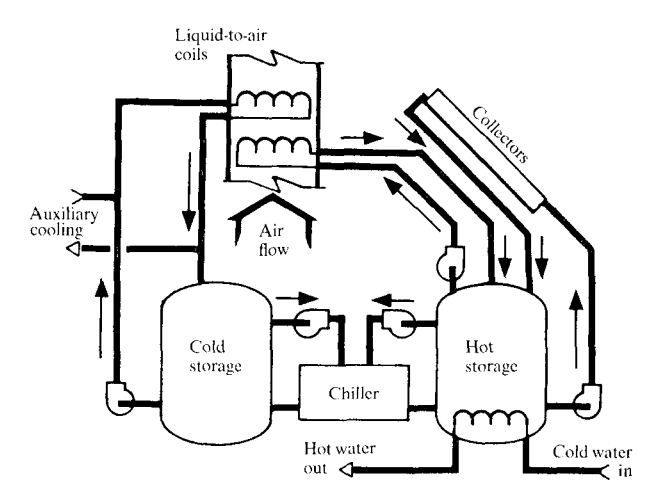


Figure 11 Schematic representation of the System F solar energy system.

heat exchangers located in the central air distribution system of the building. Auxiliary cooling is provided by supplemental cold water from a fossil-fuel-powered central chiller plant. The system, shown schematically in Fig. 11, has five modes of operation:

- Collector to storage,
- Storage to space heating,
- Domestic hot water heating,
- Chilled water production,
- Space cooling.

The performance of the system has been evaluated from March to August of 1978. Detailed reports of the thermal performance of the entire system can be found in Refs. [20, 21]. The system provided 100% of the DHW requirements, and 34% of the space cooling demand during the report period. Space heating was not required.

• Collector array performance

Table 11 summarizes the performance of the collector array for the report period. The average collector array efficiency during the report period was 15%, based on total incident solar energy. Here, the operational collector efficiency is defined by Eq. (6),

$$OCE = Q_{c}/[Q_{op}(A_{T}/A_{G})], \tag{6}$$

where $Q_{\rm c}$ is the collected solar energy, $Q_{\rm op}$ is the operational solar energy, $A_{\rm T}$ is the collector aperture area, and $A_{\rm c}$ is the gross array area.

The average operational collector efficiency was 22%. These efficiencies show a gradual deterioration from a high of 26% in May to a low of 18% in June, followed by

slight improvements in July and August. This gradual decrease in efficiency is attributed to a deteriorating suntracking sensor, a problem that was identified in early June. Attempts to restore the efficiency to former levels finally resulted in the complete redesign and installation of the collector array tracking sensor. This was accomplished on August 15 and the evaluation of the new tracker is continuing. The operational efficiencies obtained, shown in Table 11, are consistent with or slightly higher than the manufacturer's supplied test data for a single collector element operated within the same temperature ranges. A comparison of the field-derived curve with the laboratory-derived curve shown in Fig. 6(f) substantiates this numerical observation.

The effects of concentration and the required high storage temperatures of the system are reflected in the distribution of operating points on the instantaneous energy curve for August, shown in Fig. 6(f). The points are greatly skewed to the right. Forty-six percent of the operating points lie between 0.26 and 0.31 ft²-h-°F/BTU (0.046 and 0.055 m²-K/W).

Summary

Data acquired by the National Solar Data Network are being converted to useful information for the solar energy system design community. The information presented relates the predicted energy gain of a collector array based on the efficiency curve for a panel to the actual energy gain observed for specific installations. Where there is close agreement, the designer is assured that his design is adequate. On the other hand, when there is a significant deviation in the performance, the designer should consider sources of parasitic heat losses.

It has been shown that the Hottel-Whillier-Bliss model developed for a solar panel usually does not adequately represent the energy gained by either the flat-plate or concentrating collector arrays studied in this paper.

The continuing thrust of this work will be directed toward development of a collector array model or simple algorithm that can accurately calculate the total energy gained by a collector array under dynamic operating conditions. The ultimate objective is to provide the solar energy industry with a tool that will allow accurate estimations of the collector area required to satisfy specific design loads. Such a tool could lead to the optimization of design methods and the minimization of system costs.

Acknowledgment

The data and results discussed in this paper were presented at the U.S. Department of Energy Solar Update Regional Conference, July, 1978. The work was spon-

sored by the Department of Energy, Office of Conservation and Solar Applications, under contract #EG-77-C-01-4049 and is part of the National Solar Energy Demonstration Program. We wish to acknowledge the help of our colleagues, V. S. Aquila, H. L. Armstrong, T. D. Lee, and C. T. Wallace, for providing detailed information on the individual solar energy systems discussed in this paper.

References and notes

- (a) E. Streed et al., "Thermal Data Requirements and Performance Procedures for the National Solar Heating and Cooling Demonstration Program," Report No. NBSIR-76-1137, National Bureau of Standards, Washington, DC, August 1976. (b) "National Program for Solar Heating and Cooling of Buildings," ERDA Report No. 76-6, Energy Research and Development Administration, now the Dept. of Energy, Washington, DC, November 1976.
- J. I. Yellott, Chairman, "Methods of Testing to Determine the Thermal Performance of Solar Collectors," ASHRAE Standard 93-77, American Society of Heating, Refrigeration, and Air Conditioning Engineers, Inc., New York, 1977
- 3. W. H. McCumber and M. W. Weston, "Analysis of Collector Array Performance from Field Derived Measurements," Proceedings of the U.S. Dept. of Energy's Solar Update, Conference No. 780701, July 1978.
- 4. H. C. Hottel and B. B. Woertz, "Performance of Flat Plate Solar Heat Collectors," *Trans. ASME*, 91-104 (1942).
- 5. A. Whillier, "Solar Energy Collection and Its Utilization for House Heating," Sc.D. Thesis, Massachusetts Institute of Technology, Cambridge, MA, 1953.
- H. C. Hottel and A. Whillier, "Evaluation of Flat Plate Solar Collector Performance," Transactions of the Conference on the Use of Solar Energy, Tucson, AZ, 1955, Vol. III, Thermal Processes, Part 2, pp. 74-104, Tucson, Arizona, 1955.
- 7. R. W. Bliss, "Plate-Efficiency Factors of Flat-Plate Solar Heat Collectors," *Solar Energy* 3, No. 4, 55-64 (1959).
- 8. A. Whillier, "Design Factors Influencing Collector Performance," Low Temperature Engineering Application of Solar Energy, American Society of Heating, Refrigeration, and Air Conditioning Engineers, Inc., New York, 1977.
- 9. J. A. Duffie and W. A. Beckman, Solar Energy Thermal Processes, John Wiley & Sons, Inc., New York, 1974.
- 10. The c_{ν} , ρ , and $f_{\rm c}$ are calculated functions of the fluid temperature at the point of flow measurement.
- W. H. McCumber, Jr., paper on System A presented at the U.S. Dept. of Energy Solar Update Conference No. 780701, July 1978.
- 12. The following are monthly performance reports on System A, February to August, 1978. Report Nos. SOLAR/1034-78/02 through -/08. All were published by the U.S. Dept. of Energy and are available from the Technical Information Center at Oak Ridge, TN.
- Monthly performance reports on System B, February to August, 1978, Report Nos. SOLAR/2008-78/02 through -/08, U.S. Dept. of Energy, Technical Information Center, Oak Ridge, TN.
- H. L. Armstrong, paper on System B presented at the U.S. Dept. of Energy Solar Update Conference No. 780701, July 1978.
- J. C. Bartlett, "Evaluation of Solar Energy Control Systems," presented at the Solar Heating and Cooling Systems Operational Results Conference, Colorado Springs, CO, Nov. 28-Dec. 1, 1978.
- Monthly performance reports for System D, May to August, 1978, Report Nos. SOLAR/1005-78/05 through -/08, U.S. Dept. of Energy, Technical Information Center, Oak Ridge, TN

- 17. T. D. Lee, paper on System D presented at the U.S. Dept. of Energy Solar Update Conference No. 780701, July 1978.
- Monthly performance reports for System E, June to August 1978, Report Nos. SOLAR/2028-78/06 through -/08, U.S. Dept. of Energy, Technical Information Center, Oak Ridge, TN.
- V. S. Aquila, paper on System E presented at the U.S. Dept. of Energy Solar Update Conference No. 780701, July 1978.
- Monthly performance reports for System F, March to August, 1978, Report Nos. SOLAR/2018-78/03 through -/08, U.S. Dept. of Energy, Technical Information Center, Oak Ridge, TN.
- C. T. Wallace, paper on System F presented at the U.S. Dept. of Energy Solar Update Conference No. 780701, July 1978.

Received October 23, 1978; revised January 10, 1979

The authors are with the IBM Federal Systems Division, 150 Sparkman Drive, Huntsville, Alabama 35805.